ELSEVIER

S0032-3861(96)00367-9

Polymer Vol. 37 No. 22, pp. 5099–5106, 1996

0032-3861/96/$15.00 + 0.00

Simulation study of phase separation caused by polymerization

B. Lin* and P. L. Taylor†

Department of Physics, Case Western Reserve University, Cleveland, OH 44106-7079, USA
(Received 20 July 1995; revised 27 November 1995)

We study phase separation in a polymerizing system by means of Monte Carlo simulation on a triangular lattice. This serves as a model for the processes occurring in the formation of polymer-dispersed liquid crystals (PDLCs). The resulting structures are dependent not only on temperature and concentration but also on the relative rates of polymerization and diffusion. The effective phase diagrams observed in the simulations can be approximated by Flory–Huggins theory when the degree of polymerization is treated as an adjustable parameter. The time-resolved structure factor is less well approximated by an expression of the Lifshitz–Slyozov type. Copyright © 1996 Elsevier Science Ltd.

(Keywords: phase separation; polymer-dispersed liquid crystal; Monte Carlo)

INTRODUCTION

Polymer-dispersed liquid crystals (PDLCs) have become a topic of recent interest[1–7] as a consequence of their wide range of potential electro-optical applications and the challenging nature of some problems in the theoretical interpretation of their formation and operation. Phase separation is the key process used in forming PDLCs, which are micron-sized droplets of low-molecular-weight liquid crystals (LC) in a polymer matrix. The phase separation process from uniform mixtures of liquid crystals and polymer precursor is essential in three commonly used techniques for producing PDLCs[1–5,7]: polymerization of the polymer precursor to form a linear (thermoplastic) or cross-linked (thermoset) matrix; quench of a mixture of a LC and a linear polymer; and evaporation of a common solvent dissolving the liquid crystal and polymer.

Phase separation processes used in making PDLC films have many advantages over other techniques for producing similar films[1,4], including control of size and uniformity of the LC droplets, application to a wide range of polymers, and simplicity and low cost in production. The droplet size, morphology, and uniformity are important factors in determining the electro-optical properties of PDLC films, and are dependent on such phase separation parameters as temperature, concentration, and polymerization rate (in polymerization-induced phase separation), cooling rate (in thermally-induced phase separation) or evaporation rate (in the solvent-induced case).

In this paper we study the phase separation process induced by polymerization in forming PDLC films. Our goal is a qualitative understanding of the effects of temperature, polymerization rate and concentration on the resulting droplet size and uniformity. To achieve this we perform a Monte Carlo simulation on a triangular lattice to simulate the polymerization-induced phase separation in an initially uniform (randomly distributed) mixture of LC molecules and polymer precursor (monomers). At this stage we do not include the anisotropy of the LC molecules, as we consider our two-dimensional system to be in a plane perpendicular to the director of the LC. That is to say, the LC molecules are assumed to be oriented out of the plane of the paper in the illustrations of phase-separating systems shown in the figures. In the course of the computation we shall obtain the phase diagrams of the polymerized and unpolymerized systems and note the variation with time of the structure factor during the polymerization process.

It has been shown experimentally[1,3] that in general the size of the LC droplets decreases with increasing cure temperature. Similarly, a higher polymerization rate (cure rate) results in smaller LC droplets[8,9]. Higher cure temperature also decreases the time for complete cure[8,9]. The morphology of the phase-separated structure is normally that of nearly spherical LC inclusions[1,2,4,7], although other structures, such as polymer balls[10] and interconnected LC structures[11], have been reported.

Phase diagrams of PDLCs have been studied experimentally by several authors[3,7,11,12], who found behaviour characteristic of an upper critical solution temperature. The phase diagram thus has a maximum temperature above which the system is in a single phase. The phase separation temperature was found to be a monotonically increasing function of the molecular weight of the matrix, and so polymerization moves upward the critical temperature curve in a temperature–concentration plot. This has also been shown using Flory–Huggins theory in a numerical calculation of the phase diagram of a LC and photocurable prepolymer system[13–15].

Time-resolved light scattering experiments are useful in studying the kinetics of the phase separation process in PDLCs. The scattered light intensity as a function of

* Present address: Department of Physics, University of Minnesota, Minneapolis, MN 55455, USA
† To whom correspondence should be addressed

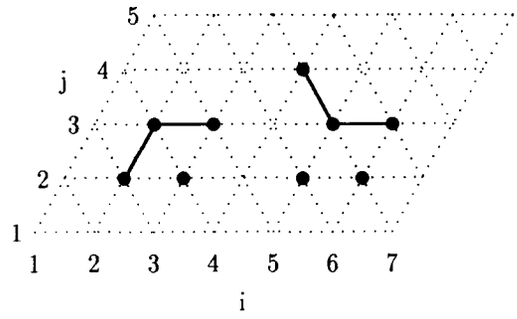

Figure 1 The triangular lattice on which the Monte Carlo simulations are performed. The solid lines represent polymer bonds

scattering angle shows a peak at an angle not equal to zero, and the peak grows and the angle decreases with time[11,16]. A sudden increase in scattered-light intensity can be used as a signature of the occurrence of an appreciable phase separation[11,16]. In other polymer systems, mostly polymer blends and polymer–solvent systems, light scattering studies of phase separation have been undertaken much more extensively both in experiment and in theory[17–22], and show many aspects of the behaviour of the structure factor that are similar to those seen in PDLC films. We now proceed to see to what extent our simulations can yield comparable results.

MONTE CARLO MODEL

The model we use to study the phase separation process in a binary mixture of low-molecular-weight liquid-crystal molecules and polymerizing monomers is a two-dimensional triangular lattice (*Figures 1–4*) with each site occupied by either a LC molecule (blue circle) or a monomer (red circle). The triangular lattice is used to simulate the close packing of molecules in an incompressible system. Liquid crystal molecules and monomers are initially randomly distributed on the lattice with probability c and $(1 - c)$ respectively, to form a uniform mixture. The lattice system is assumed to obey periodic boundary conditions in two directions in order to minimize the boundary effects of a finite-size system. Most of the calculations are done on a lattice of size 40×40, although some larger systems with sizes up to 80×80 are also examined to check for size effects. Symmetric nearest-neighbour interactions act between LC molecules and monomers, with the intermolecular interaction energy ϵ defined to be,

$$\epsilon = \begin{cases} 1 & \text{different neighbouring molecules} \\ 0 & \text{like neighbouring molecules} \end{cases} \quad (1)$$

To see the effects of polymerization on the process of phase separation, the time evolution of both polymerizing and non-polymerizing systems are studied.

Non-polymerizing systems

In these systems, the monomers remain unpolymerized during the process of phase separation. This corresponds to the uncured LC/matrix systems[7,13]. It is initially a uniform mixture of LC molecules and monomers, and is then quenched to a temperature T (measured in units of ϵ/k_B) and evolves according to a standard Monte Carlo procedure as follows:

(a) Randomly select a site (i,j) and one of its six nearest neighbours, (i_n,j_n). Here i is the column index and j the row index of the triangular lattice (*Figure 1*).
(b) Evaluate the energy difference $\Delta E = E_2 - E_1$ of the system between the energy $E_2(i_1 j_1, \ldots, i_n j_n, \ldots, ij, \ldots)$ of the new state formed by exchanging occupancies of the two sites (i, j) and (i_n,j_n), and the energy $E_1(i_1 j_1, \ldots, ij, \ldots, i_n j_n, \ldots)$ of the original state. Since the two sites involved are nearest neighbours, and the intermolecular interactions also involve only nearest neighbours, the energy difference ΔE due to interchange involves only the 10 sites surrounding and including the two sites.
(c) Update according to the rule that if $\Delta E \leq 0$ the exchange between (i,j) and (i_n,j_n) is made, but if $\Delta E > 0$ then the exchange is made only if $e^{-\Delta E/T} > R$, where R is a random number between 0 and 1, and is changed each time this step is executed.
(d) Repeat the procedure: two new neighbouring sites are randomly selected and the system is again updated.

Polymerizing systems

We consider the situation in which the monomers can polymerize bifunctionally, so that each monomer can be bonded to at most two other monomers. Once formed between nearest-neighbouring monomers, a bond is considered unbreakable. However, in order to allow some mobility to the polymerized molecules we make the bond extensible up to the distance between next-nearest neighbours, and permit exchanges at this distance. We impose no energy cost for this extension. The interaction between unlike molecules remains restricted to nearest neighbours.

To the Monte Carlo process for the non-polymerizing system described above, a polymerization process is added for monomers only. The system starts as before with a random distribution of LC molecules and monomers, and then utilizes the following procedure:

(a) Randomly select a site (i, j) and one of its twelve nearest and next-nearest neighbours, (i_n,j_n).
(b) Evaluate the energy difference ΔE after and before exchanging (i, j) and (i_n,j_n), as in the non-polymerizing system. There are now up to 12 sites involved in the change of configuration due to the exchange.
(c) Update in the same way as in the non-polymerizing systems section, so that the exchange between (i, j) and (i_n,j_n) is made only when $e^{-\Delta E/T} > R$. Note however, that because of the polymerization of monomers, the exchange procedure is more restricted than before. If sites (i, j) and (i_n,j_n) are both occupied by LC molecules or by unpolymerized monomers, then the exchange between them is still only governed by the energy difference (and a random number) as described. If, however, one or both sites are occupied by polymerized monomers, then the exchange between these two sites is also restricted by polymer bonds: an exchange of two molecules cannot be made if it would break the existing polymer bonds. A polymer bond can be extended to next-nearest neighbours, but beyond that the bond is considered broken. For the configuration shown in *Figure 1*, for example,

Figure 2 A snapshot of the Monte Carlo simulation in a non-polymerizing system of LC molecules (blue circles), with concentration $c = 0.4$, and monomers (red circles) after some thermalization. At the high temperature $T = 2.5$ little phase separation is observed

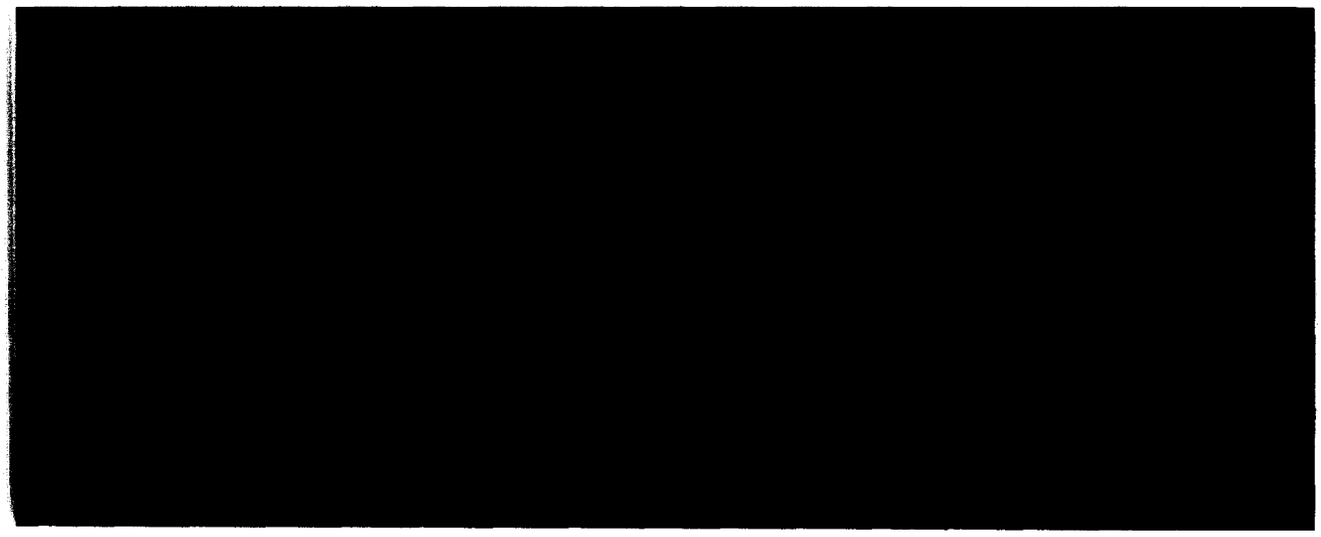

Figure 3 The same system as in *Figure 2* at a lower temperature $T = 1.2$ (below the critical temperature $T_c = 1.75$). Phase separation occurs and nearly circular regions of blue circles are seen

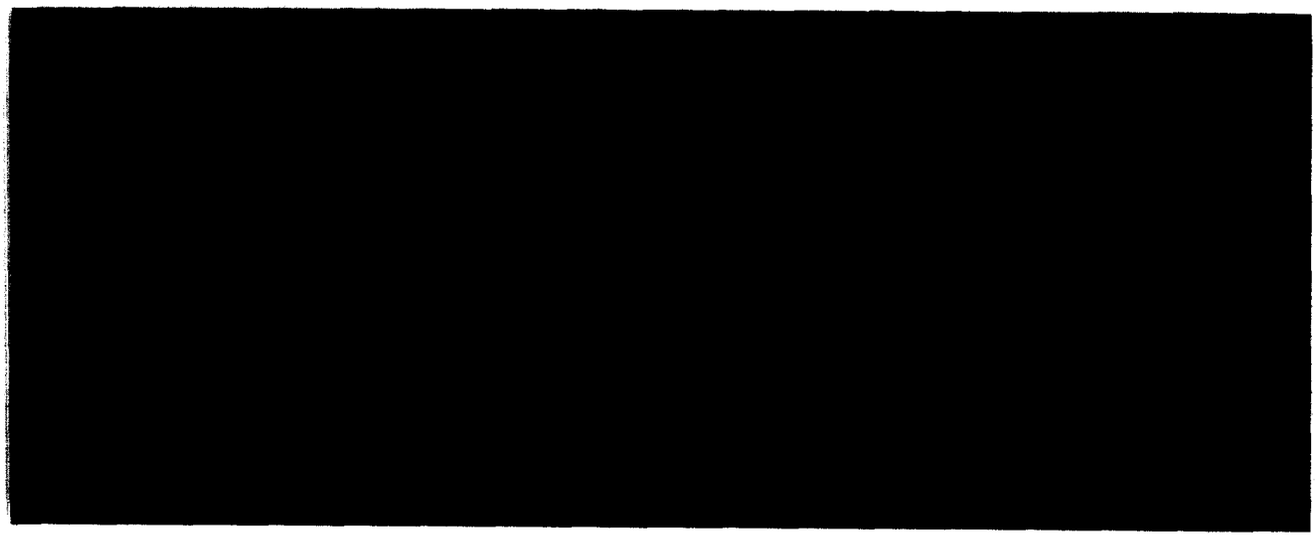

Figure 4 A polymerizing system with $c = 0.4$ and $K_p = 0.5$. The system is at the same high temperature $T = 2.5$ as in *Figure 2*, but polymerization causes phase separation

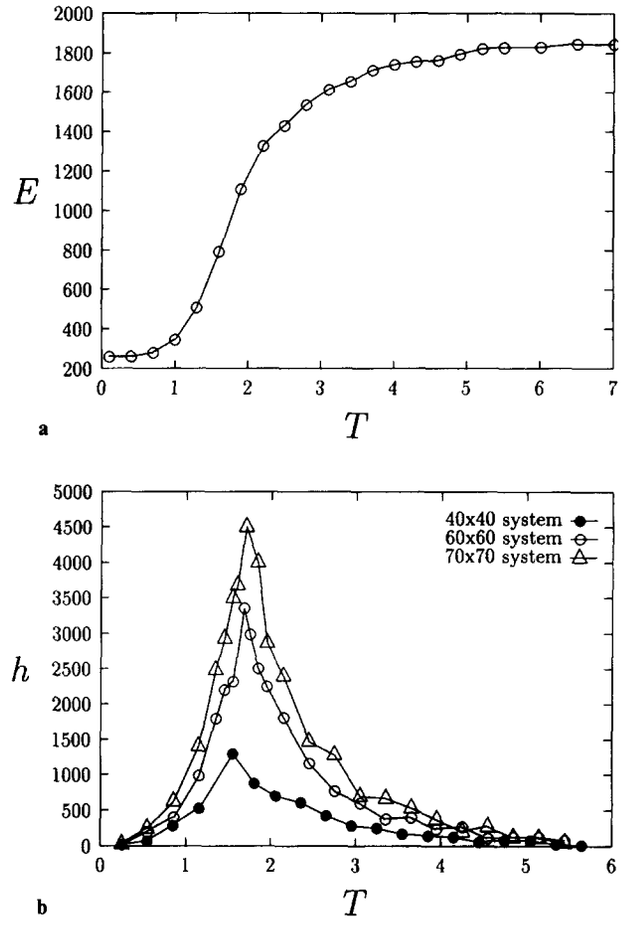

Figure 5 (a) Equilibrium energy E, shown as a function of temperature T for a 40 × 40 non-polymerizing system $c = 0.3$, has a sharp increase around $T = 1.6$. (b) The specific heat h as a function of T for three non-polymerizing systems with $c = 0.5$ and sizes of 40 × 40, 60 × 60 and 70 × 70. The tendency of h is to diverge as the system is increased confirms the expected singularity in the specific heat at $t = 1.75$ for this concentration

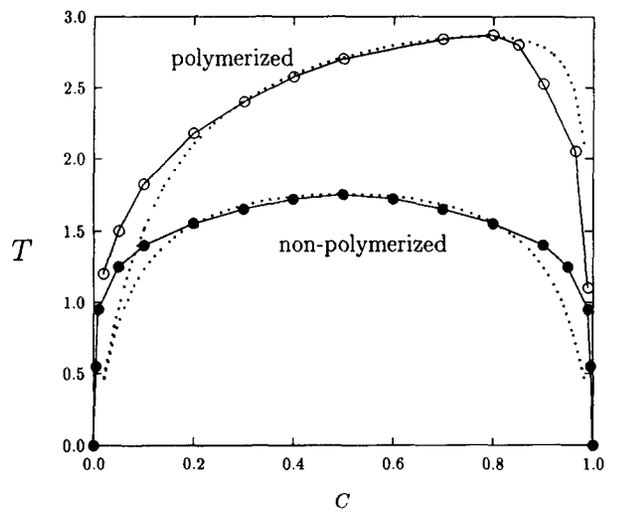

Figure 6 The phase diagram for polymerizing and non-polymerizing systems. Polymerization raises the phase separation temperature and shifts the critical concentration to a larger c value. The dotted curves are fits to Flory–Huggins theory. The polymerizing systems have $K_p = 0.1$

molecules on site (5, 3) and (6, 2) cannot be exchanged because that will break the polymer bond between site (4, 4) and site (5, 3). An exchange between (5, 3) and (5, 2), however, is possible.

(d) After each actual or attempted exchange between sites (i, j) and (i_n, j_n), try to polymerize site (i, j) with one of its randomly selected nearest or next-nearest neighbours. This polymerization attempt is made successfully with a probability K_p, the polymerization rate, and is subject to the following restrictions:

1. Sites (i, j) and its randomly selected neighbour (i_p, j_p) must both be occupied by monomers.
2. Each of the two monomers must have fewer than two polymerization bonds. Once a monomer polymerizes with another monomer, a polymer bond (a yellow bond in *Figure 4*) is constructed between them. In *Figure 1* the monomer at site (3, 2) cannot polymerize with the one at (2, 3), which already has two bonds connected to it. It can, however, polymerize with the one at site (2, 2), for example, if the other conditions are satisfied. This bifunctional polymerization process is intended to represent the thermoplastic polymers.

(e) Repeat the procedure from (a) to (d).

In both polymerizing and non-polymerizing systems, time-resolved and equilibrium aspects of the phase separation process were studied. When examining the equilibrium properties of the systems, we discarded the first 10^8 Monte Carlo time steps at high temperatures. At low temperatures, the system reaches its equilibrium much more slowly, and we correspondingly increased the relaxation time to 10^9–10^{10} steps to allow it to equilibrate. Calculations were made by averaging data over 20 runs with different random initial configurations and over configurations measured at 500 different times after equilibrium was reached in each run.

NUMERICAL RESULTS

Phase separations

One of the important effects of polymerization on phase separation is an increase in the phase separation temperature T_c determined by the coexistence curve in the phase diagram. *Figure 2* shows a snapshot of the Monte Carlo simulation of a 40 × 40 non-polymerizing system. From an initially randomly distributed mixture of LC molecules (blue circles) with concentration $c = 0.4$ and monomers (red circles) the system is approaching equilibrium. The temperature $T = 2.5$ chosen for this system is above the critical temperature T_c, which at this concentration is only about 1.75. The operating point thus lies in the one-phase region of the phase diagram. The time steps in the figure are measured as the number of attempted Monte Carlo exchanges. We see that at this high temperature, little phase separation occurs, and the system's energy remains elevated. As the temperature is lowered to below the critical temperature, a phase separation occurs, as shown in *Figure 3*, where well-defined, nearly circular regions of blue circles are observed. The effect of polymerization on the phase-transition temperature can be seen in *Figure 4*, in which monomers (red circles) have polymerized, as indicated by the yellow polymer bonds. We see that at the same high temperature, $T = 2.5$, as that in the uncured system in *Figure 2*, the polymerization has caused phase separation. We also see from the figure that the energy of the

system is much lower than that in the uncured system. The increase in the critical temperature in polymerizing systems is due to the decrease in entropy of monomers whose motion is restricted by chemical bonds. This will now be discussed quantitatively in terms of the relevant phase diagrams.

Phase diagram

The phase diagram of both polymerizing and non-polymerizing systems was formed from the variation of equilibrium energies with temperature. System energies were calculated numerically for each temperature after the systems had reached their equilibria, and thence the specific heats were also calculated as functions of temperature by numerical differentiation. *Figure 5a* shows the equilibrium energy as a function of temperature for a non-polymerizing system with LC concentration $c = 0.3$. The specific heat of the system is shown in *Figure 5b* for $c = 0.5$ and three different system sizes. The energy in *Figure 5a* shows a sharp increase at a temperature around 1.6, and in *Figure 5b* we see a peak in the specific heat at the corresponding temperature as expected from the equivalence of this system to an Ising ferromagnet. To illustrate the comparative insensitivity of the computation to changes in the size of the lattice, we plot three specific-heat curves with system sizes of 40×40, 60×60 and 70×70, and note the small changes in location of the singularity. A phase diagram was constructed for both polymerizing and non-polymerizing systems (*Figure 6*) using critical temperatures obtained from the specific-heat singularity. For the polymerizing systems, a polymerization rate of $K_p = 0.1$ was used. Similar phase diagrams have been obtained from some experiments[3,12,18].

For comparison the commonly used Flory–Huggins approximation for the coexistence curve is shown in *Figure 6* as a pair of dotted curves. These two curves were calculated from the relations[14]

$$\chi = \left[\ln\frac{c}{c'} - \frac{1}{m}\ln\frac{1-c}{1-c'}\right] \Big/ [2(c-c'] \qquad (2)$$

and

$$2(1-m)(c-c') + (2-c-c')\ln\left(\frac{1-c}{1-c'}\right) + m(c+c')\ln\left(\frac{c}{c'}\right) = 0 \qquad (3)$$

where m is the degree of polymerization of the polymer and χ is the interaction parameter between LC and polymer and is taken to be of the form $\chi = A + B/T$. The parameters A and B in the expression for χ were chosen to be $A = -5$ and $B = 15$ in order to obtain the best fit to the lower dotted curve, for which $m = 1$. The upper dotted curve was produced by choosing the value of m as 12 in order to fit the critical temperature indicated by the data. One sees that the Flory–Huggins approximation provides a reasonable fit to the polymerized system if one can make the right guess as to the effective degree of polymerization.

Growth of liquid-crystal droplets

In the absence of polymerization, the prediction of the rate of growth of droplets reduces to a well-studied problem. For times that are neither too short nor too long one expects a result of the Lifshitz–Slyozov form[23],

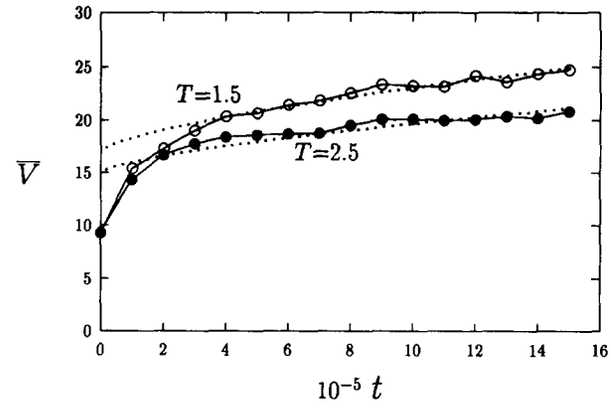

Figure 7 Averaged droplet size $\bar{V}$ as a function of time t for a polymerizing system with $c = 0.3$ and $K_p = 0.1$. The droplet curves are fits to a modified Lifshitz–Slyozov expression

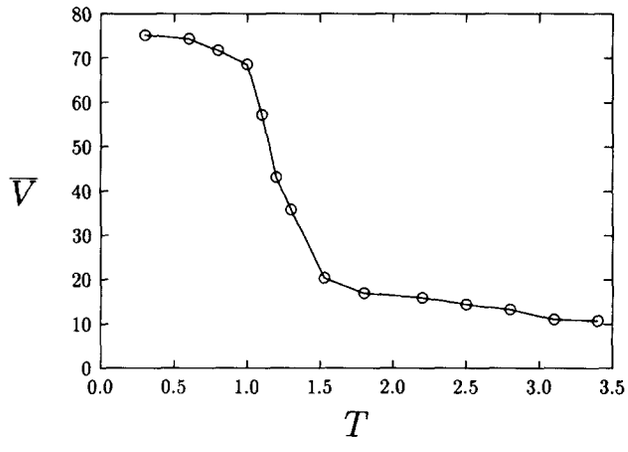

Figure 8 The averaged droplet size $\bar{V}$ for a non-polymerizing system with $c = 0.2$ shows a sharp decrease near the critical temperature

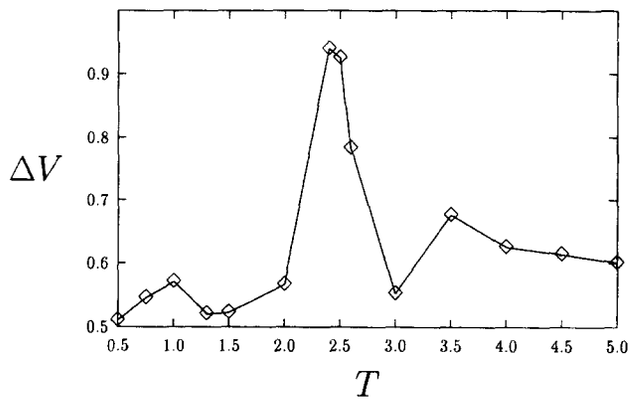

Figure 9 The size deviation ΔV as a function of temperature T for a polymerizing system with $c = 0.3$ and $K_p = 0.1$. A large deviation in droplet size is seen near the critical temperature $T_c = 2.4$

in which the typical droplet diameter D grows as $t^{1/3}$. An obvious question to ask is how this result is modified in a polymerizing system.

Before examining the results of the simulation, however, we pause to note some expected limitations in the interpretation in terms of simple expressions for the rate of growth of droplets. The energy is, in our model, due entirely to the interaction between unlike molecules on neighbouring sites, and is thus a measure of the total length of the boundaries separating regions of pure liquid crystal from pure polymer. Because the transition

that occurs when the coexistence curve is crossed is of second order, neither the energy nor its derivative with time is discontinuous. This means that it is impossible to tell by eye the difference between two configurations formed in simulations marginally below and above the transition temperature.

In discussing the size of 'droplets' we note that the irregularly shaped inclusions of pure material we identify are different from the spherical domains of homogeneous mixture that form the basis of many theories of coarsening. We nevertheless make the approximate connection between the two approaches. The diameters D of the 'droplets' seen in a two-dimensional model will scale as the (non-fractal) lengths of their perimeters and hence as the energy divided by the number N_0 of droplets. To conserve the total number of LC molecules we must have $N_0 D^2$ approximately constant. This leads to the conclusion that $D \propto E^{-1}$.

The simulations to determine the rate of growth of droplet size were performed by starting a binary system at a uniform mixture by randomly distributing LC molecules and monomers. The system was then quenched to the desired temperature and allowed to evolve by the Monte Carlo procedure described earlier. The LC droplets are seen to grow rapidly as the phase separation begins, and then to grow more slowly as equilibrium is approached. *Figure 7* shows the averaged droplet size $\bar{V}$ as a function of time for a polymerizing system with $c = 0.3$ and $K_p = 0.1$. The size $\bar{V}_i$ of a droplet is defined as the number of LC molecules inside the droplet, and $\bar{V}$ is then simply

$$\bar{V} = \frac{1}{N_0} \sum_{i=1}^{N_0} V_i \tag{4}$$

where N_0 is the total number of droplet clusters with at least five LC molecules, and V_i the size of the ith droplet. The relative size deviation ΔV used to measure the uniformity of droplets is defined as

$$\Delta V = \frac{1}{N_0} \sum_{i=1}^{N_0} \frac{| V_i - \bar{V} |}{\bar{V}} \tag{5}$$

Because the results of our simulation are obviously not in agreement with the standard Lifshitz–Slyozov relation $V = at^{2/3}$, we have attempted to fit the data to the so-called modified Lifshitz–Slyozov law[21] of the form $V = a + bt^{2/3}$, shown as dotted lines in *Figure 7*. For $t > 6 \times 10^5$ a passable agreement is seen.

The dependence of the averaged droplet size on temperature can be seen in *Figure 8* for a non-polymerizing system with $c = 0.2$. We see not only an increase in droplet size with decreasing temperature, but also a rapid increase in the rate of the size increase near the critical temperature (about 1.5 in this case). This confirms the inverse relation between energy and droplet size, and is also a signature of the phase separation. Similar behaviour of droplet size has been observed in experiments[3,4].

The depth of quench influences the size distribution of droplets in systems of low molar mass, and a similar effect is seen in the polymerizing systems. *Figure 9* shows the size deviation ΔV for a polymerizing system with $c = 0.3$ and $K_p = 0.1$ as a function of temperature. At low temperatures, which correspond to a deep quench, the droplet size is fairly uniform, as it is at high

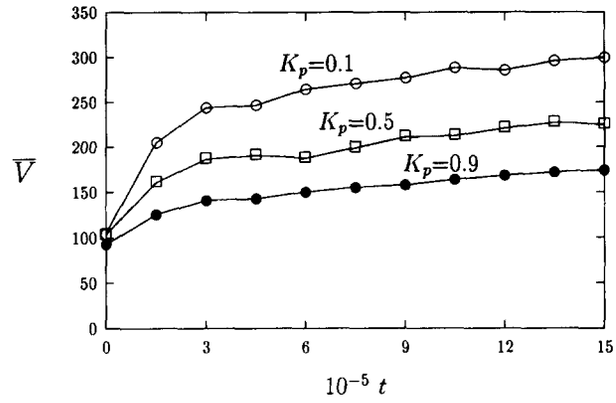

Figure 10 The effect of polymerization rate K_p on the averaged droplet size $\bar{V}$. Shown are three systems with $c = 0.5$, $T = 1.0$, and $K_p = 0.1, 0.5$ and 0.9, respectively

temperatures above the transition point. It is only at temperatures close to the transition point (about $T_c = 2.4$ in this case) that large variations in droplet size are seen.

We have used both polymerizing and non-polymerizing systems in our calculations of the dependencies of droplet-size growth rate, equilibrium size and size uniformity on temperature and concentration. The behaviour of these dependencies is similar in both types of system, although the critical temperatures are different.

The effect of polymerization rate K_p on LC droplet size is shown in *Figure 10*. A larger K_p leads to smaller averaged droplet size. This is as expected, since fast polymerization seals small LC droplets before they can grow larger. This fast curing effect on droplet size has been observed in some experiments[24–26], where the cure rate was controlled by changing the intensity of incident ultraviolet light. Our numerical calculations also indicate that a smaller K_p produces more uniform droplets.

Structure factor

Structure factors of polymer–polymer and polymer–solvent systems on simple cubic lattices have been calculated by some authors[19,21]. We will similarly calculate the time-resolved structure factor for our two-dimensional PDLC system on a triangular lattice. The structure factor $S(\vec{q}, t)$ for LC molecules is

$$S(\vec{q}, t) = \langle \frac{1}{N_l} \sum_{\vec{r}} \sum_{\vec{r}'} e^{i\vec{q}\cdot(\vec{r}-\vec{r}')} [\phi(\vec{r}, t)\phi(\vec{r}', t) - c^2] \rangle$$

$$\vec{q} = (\frac{2\pi}{N})(n_i, n_j) \text{ with } n_i, n_j = 0, 1, \ldots, N-1 \tag{6}$$

where N_l is the total number of LC molecules, $N \times N$ the total number of lattice sites and $c = \langle \phi \rangle$. The summations run over the whole lattice, and the average $\langle\ \rangle$ is the configurational average. Equation (6) can be written in a more practical form as

$$S(\vec{q}, t) = \langle \frac{1}{N_l} \left[\left(\sum_{\vec{r}} \cos(\vec{q}\cdot\vec{r}) \right)^2 + \left(\sum_{\vec{r}} \sin(\vec{q}\cdot\vec{r}) \right)^2 \right] \rangle - c^2 N_l \delta_{\vec{q}0} \tag{7}$$

where $\sum_{\vec{r}}$ sums over LC molecules only.

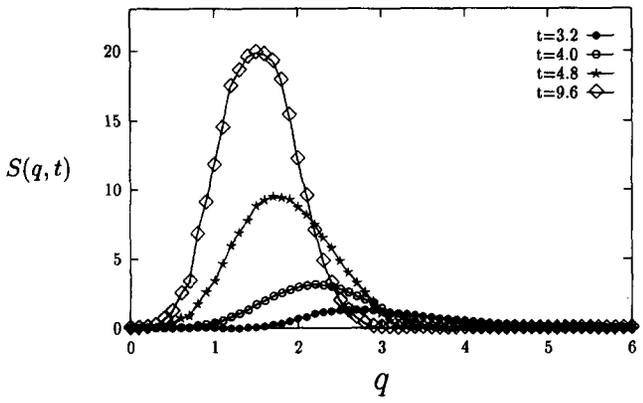

Figure 11 The time-resolved structure factor $S(q, t)$ for a polymerizing system with $c = 0.3$, $K_p = 0.1$ and $T = 2.3$. The peak of $S(q, t)$ increases and the q position for the peak decreases as the phase separation progresses. The time indicated in the figure is in units of 10^5 steps

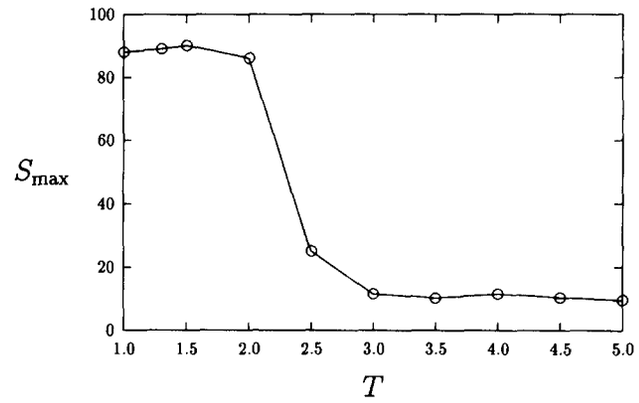

Figure 12 Plot of the maximum, S_{max}, of the structure factor as a function of temperature T for a polymerizing system with $c = 0.3$ and $K_p = 0.1$

Because our simulation is performed on a triangular lattice our results for $S(\vec{q}, t)$ are comparatively free of the anisotropy that is an artifact of the use of square or cubic lattices. We nevertheless average over directions of $\vec{q}$ in the manner suggested in ref. 21. That is, we define a spherically averaged structure factor $S(q, t)$,

$$S(q,t) = \frac{1}{n_q} \sum_{q=q-\Delta q/2}^{q+\Delta q/2} S(\vec{q}, t) \qquad (8)$$

where $n_q = \sum_{q=q-\Delta q/2}^{q+\Delta q/2} 1$, where $q = |\vec{q}|$, and Δq is chosen to be $2\pi/N$.

The time resolved structure factor defined in equation (8) for a polymerizing system with $c = 0.3$, $K_p = 0.1$ and $T = 2.3$ is shown in *Figure 11*. A similar structure factor is also seen for non-polymerizing systems. We see that as the phase separation progresses the peak of $S(q,t)$ grows and the q value at the peak, q_{max}, decreases. This behaviour of $S(q,t)$ has been observed in PDLC experiments[16], although the decrease in q_{max} in our model is not as large as in one of the experiments. Similar behaviour was also reported in polymer blend experiments[17,18] and in numerical studies of polymer–solvent and polymer blend systems[19,21]. *Figure 12* shows the temperature dependence of the equilibrium maximum of the structure factor, S_{max}. For a polymerizing system with $c = 0.3$ and $K_p = 0.1$, we see again that S_{max} has a large decrease near the critical temperature. The large-q tail of the structure factor decays more rapidly than would be expected from the Porod-law prediction[27] of q^{-3} for two-dimensional systems, but this is probably not significant, given the small size of the sample.

CONCLUSION AND DISCUSSION

In this two-dimensional set of simulations of a system undergoing phase separation we have seen that the observed structures are qualitatively similar to what one might expect on the basis of some simple theories. The details of this behaviour, however, are not described well by these models. The polydispersity of the molecules formed in the polymerization process must be expected to lead to deviation from Flory-Huggins theory, and this is indeed observed at low and high concentrations.

The use of a triangular lattice (rather than the square lattice traditionally favoured for its ease of implementation) results in a structure that has comparatively low anisotropy. This should mean that our calculations of droplet size will be more meaningful than those produced from simpler models, and hence more relevant to predictions concerning PDLC films. We find that higher temperatures, larger polymerization rates or smaller LC concentrations all lead to smaller LC droplets. Droplet size was found to be least uniform near phase separation temperatures.

The time-resolved structure factor $S(q, t)$ showed an increase in its maximum and a decrease in the position of the dominant wavenumber as time increased. While these results are expected on the basis of Lifshitz–Slyozov theory, the rate of growth of droplet size is apparently further reduced by the lowered mobility of the growing polymers. The relatively long inception time for phase separation experimentally observed in ref. 16, however, was not seen in our calculations: the LC droplets and structure factor in our model start to grow very quickly after quench or polymerization begins. We bear in mind, however, that the dimensionality of the system is important, and that a three-dimensional model might yield different behaviour.

ACKNOWLEDGEMENTS

This work was supported by the National Science Foundation at the ALCOM Science and Technology Center funded by Grant Number DMR89-20147, and made use of the resources of the Ohio Supercomputing Center. One of us (PLT) thanks Professor A. H. Windle and the Department of Materials Science and Metallurgy of the University of Cambridge for their hospitality while part of this work was performed.

REFERENCES

1 Doane, J. W., Golemme, A., West, J. L., Whitehead, J. B. and Wu, B.-G. *Mol. Cryst. Liq. Cryst.* 1988, **165**, 511
2 Doane, J. W. in 'Liquid Crystals — Applications and Usages' (Ed. B. Bahadur)', Vol. 1, World Scientific, 1990, p. 361
3 West, J. L. *Mol. Cryst. Liq. Cryst.* 1988, **157**, 427
4 West, J. L. in 'Liquid-crystalline Polymers' (Eds R. A. Weiss and C. K. Ober), American Chemical Society, 1990, p. 475
5 Kitzerow, H.-S. *Liq. Cryst.* 1994, **16**, 1
6 Montgomery, G. P. in 'Large Area Chromogenics: Materials and

Devices for Transmittance Control' (Eds C. M. Lampert and C. G. Granqvist), SPIE Optical Engineering Press, 1990, p. 577
7 Smith, G. W. *Int. J. Mod. Phys. B* 1993, **7**, 4187; *Mol. Cryst. Liq. Cryst.* 1994, **239**, 63
8 Smith, G. W. and Vaz, N. A. *Liq Cryst.* 1988, **3**, 543
9 Smith, G. W. *Mol. Cryst. Liq. Cryst.* 1990, **180B**, 201
10 Yamagishi, F. G., Miller, L. J. and van Ast, C. I. *Proc. SPIE* 1989, **1080**, 24
11 Kyu, T., Mustafa, M., Yang, J., Kim, J. Y. and Palffy-Muhoray, P. in 'Polymer Solutions, Blends, and Interfaces' (Eds I. Noda and D. N. Rubingh), Elsevier, 1992, p. 245
12 Smith, G. W. *Phys. Rev. Lett.* 1993, **70**, 198; *Mol. Cryst. Liq. Cryst.* 1993, **225**, 113
13 Hirai, Y., Niiyama, S., Kubai, H. and Gunjima, T. *Proc. SPIE* 1990, **1257**, 2
14 Nishi, T. *J. Macromol. Sci. – Phys.* 1980, **B17**, 517; *CRC Crit. Rev. Solid State Mater. Sci.* 1985, **12**, 329
15 Shen, C. and Kyu, T. *J. Chem. Phys.* 1995, **102**, 556
16 Kim, J. Y. and Palffy-Muhoray, P. *Mol. Cryst. Liq. Cryst.* 1991, **203**, 93
17 Okada, M. and Han, C. C. *J. Chem. Phys.* 1995, **85**, 5317
18 Cumming, A., Wiltzius, P., Bates, F. S. and Rosedale, J. H. *Phys. Rev. A* 1992, **45**, 885
19 Rodriguez, A. L., Freire, J. J. and Horta, A. *J. Phys. Chem.* 1992, **96**, 3954
20 Wang, Z.-Y., Konno, M. and Saito, S. *J. Chem. Phys.* 1989. **90**, 1281
21 Chakrabarti, A., Toral, R., Gunton, J. D. and Muthukumar, M. *J. Chem. Phys.* 1990, **92**, 6899
22 Sciortino, F., Bansil, R. and Stanley, H. E. *Phys. Rev. E* 1993, **47**, 4615
23 Lifshitz, I. M. and Slyozov, V. V. *J. Phys. Chem. Solids* 1961, **19**, 35
24 Montgomery, G. P., Vaz, N. A. and Smith, G. W. *Proc. SPIE* 1988, **958**, 104
25 Smith, G. W. *Mol. Cryst. Liq. Cryst.* 1991, **196**, 89
26 Lackner, A. M., Margerum, J. D., Ramos, E. and Lim, K.-C. *Proc. SPIE* 1989, **1080**, 53
27 Porod, G. in 'Small-angle X-ray Scattering' (Eds O. Glatter and O. Krattky), Academic Press, New York, 1982